ISSN 1061-9348, Journal of Analytical Chemistry, 2014, Vol. 69, No. 6, pp. 590–597. © Pleiades Publishing, Ltd., 2014.
Original Russian Text © N.S. Medvedev, A.R. Tsygankova, V.F. Kukarin, A.I. Saprykin, 2014, published in Zhurnal Analiticheskoi Khimii, 2014, Vol. 69, No. 6, pp. 652–659.

ARTICLES

Possibilities of Inductively Coupled Plasma Atomic Emission Spectrometry with Electrothermal Vaporization in the Analysis of High-Purity Reagents

N. S. Medvedev, A. R. Tsygankova, V. F. Kukarin, and A. I. Saprykin

Nikolaev Institute of Inorganic Chemistry, Siberian Branch, Russian Academy of Sciences, pr. Akad. Lavrent'eva 3, Novosibirsk, 630090 Russia
e-mail: medvedev@niic.nsc.ru, saprykin@niic.nsc.ru

Received April 26, 2013; in final form, September 23, 2013

Abstract—Possibilities of electrothermal sample vaporization in inductively coupled plasma atomic emission spectrometry (**ETV-ICP-AES**) in the analysis of high-purity reagents were studied on an example high-purity waters, acid solutions, and trace impurity concentrates. The analytical and background signals in the injection of solutions into inductively coupled plasma (**ICP**) by pneumatic nebulization and electrothermal vaporization were compared and the of limits of detection in the analysis of high-purity reagents with impurity preconcentration by evaporation were estimated and compared.

Keywords: electrothermal vaporization, analysis of solutions, atomic emission spectrometry, inductively coupled plasma

DOI: 10.1134/S1061934814040066

Preconcentration is an efficient method for reducing the limits of impurity detection in the analysis of high-purity substances and materials by ICP AES [1]. Trace impurities in the analysis of solid samples of high-purity substances are usually preconcentrated by the distillation of sample matrix [2–4] and, in the analysis of solutions, by evaporation [5, 6]. The impurity concentrate after the distillation of sample matrix is a solid substance of the weight no more than 1 mg or a solution of the volume no more than 10 μL. In pneumatic nebulization, no less than 2 mL of a solution is required for two or three replicate measurements by ICP-AES, which makes necessary a 100- and even a 1000-fold dilution of the concentrates in their transfer into a solution because of the low efficiency (no more than 2%) of the pneumatic nebulization of solutions into ICP using standard nebulization systems [7]. The high degree of dilution of sample concentrates results not only in the reduction of the analytical signal (**AS**) of impurity elements, but also in an increased probability of uncontrolled pollution. As a rule, in preparing solutions for ICP AES, analysts use high-purity grade acids additionally purified by distillation below the boiling point (for example, HNO_3, HCl, HF) and deionized water. The purity of the reagents used in the ICP AES analysis determines the value of the blank experiment (**BE**), the reproducibility of the results of analysis, and the attained values of the limits of detection (**LOD**).

Electrothermal vaporization is an alternative method for the injection of small sample volumes into ICP. For one ETV-ICP-AES analysis only several microlitres of a solution should be taken, which allows an analyst to exclude the step of concentrate dilution. For example, as was shown in [8, 9], the use of electrothermal vaporization ensures on an average a tenfold reduction of LOD for analytes in solutions in comparison with ICP AES analysis with pneumatic nebulization of solutions. The LOD for Al, Cu, Fe, Mg, Mn, S, Se, Si, and Zn in the ETV-ICP-AES analysis of aqueous solutions varies from 1×10^{-8} to 4×10^{-6} wt %.

The aim of this work was the study and choice of the optimum parameters of electrothermal vaporization and inductively coupled plasma and the estimation of the performance characteristics of ETV-ICP-AES as applied to the analysis of high-purity reagents with preconcentration by impurity evaporation on an example of analysis of high-purity nitric acid grade 27-5.

EXPERIMENTAL

Instruments. We used a ThermoScientific ICP-AES spectrometer series iCAP-6500 Duo with standard equipment for sample injection into ICP and a peristaltic pump. The working parameters of the spectrometer are listed in Table 1. In the measurements we used axial observation of ICP, which ensured a higher analytical signal compared to the radial mode. Small volumes of solutions were injected using a P.S. Analytical 60.800 electrothermal vaporizer (Great Britain); its scheme is presented in Fig. 1.

Table 1. Spectrometer parameters

ICP parameters	
Power of high-frequency generator, W	750–1350
Argon pressure in the spectrometer blowing line, kPa	650
Auxiliary argon flow rate, L/min	0.5
Cooling argon flow rate, L/min	12
Plasma observation	Axial
Signal recording, s	10
Parameters of solution delivery though an pneumatic nebulizer	
Flow rate of solution delivery with a peristaltic pump in washing, mL/min	3
Washing time, s	30
Time of peristaltic pump stabilization, s	5
Flow rate of solution delivery with a peristaltic pump in measurements, mL/min	1.5
Argon nebulizing flow rate, L/min	0.6

A graphite cell was fixed in water-cooled holders (Fig. 1, *4*) with an attached power supply unit (Fig. 1, *7*). The transporting flow of high-purity argon (TU 6-21-12-94) was blown from the cell bottom at a controlled rate in the 0–2.5 L/min. The cell was heated by electric current and the vaporized sample components arrived at the ICP through a fluoroplastic pipe 50 cm in length and 4 mm in inner diameter. Using an adjustable power supply unit of the ETV, the cells could be heated according to a temperature program including up to four steps, each up to 99 s long. The temperature of the cell in the range from room temperature to 2400°C was set by the value of the supplied voltage, from 0 to 17 V. Before the measurements, an aliquot portion of a solution (25 μL) was transferred into the cell with a microdosing unit and then a temperature program was started.

Reagents and solutions. We used 14 M high-purity HNO_3 brand 27-5 and water twice-distilled under the boiling point (DuoPUR, Milestone) and deionized with a resistance of 18.2 MΩ (Direct-Q3, Millipore). Solutions were prepared using standard Slope multielement solutions (**MES**), Novosibirsk, Russia. The concentrations (μg/mL) of elements in the MES were as follows: MES 1, Al, Ca, Cd, Cr, Fe, Mg, Mn, Na, Zn (each 50), K (37.5), and P (67.4); MES 2, B, Bi, Co, Cu, Ga, In, Ni, Si, Ti, V (each 50), and Na (81.9); MES 3, As, Pb, Rb, Sb, Se, Sn, Te (each 50) and Ag, Ba, Be, Sr (each 20); and MES 4, Hf, Mo, Nb, Re, Ta, W, Zr, (each 50).

To optimize the transporting gas flow, select the power of the ICP, and quantitatively determine analytes arriving at the ICP under the used temperature program, we prepared multielement solutions from MES solutions with concentrations of the majority of analytes 1 μg/mL.

RESULTS AND DISCUSSION

Optimization of ETV program. The temperature program in electrothermal vaporization includes four successive steps: sample drying, pyrolysis, analyte vaporization, and purification. Heating the cell at the drying step should ensure efficient solvent evaporation with the least analyte losses. If the sell is heated too strongly, the evaporation of the solvent can be intensive and lead to losses [8]. To select voltage at the step of sample drying, 25 μL of distilled water was placed in a cell with a microdosing unit and then voltage in the range from 1.5 to 2.3 V was applied across the cell. Voltage of ≈1.8 V was found to be optimum. In this case, 25 μL of a solution was nebulized for 35–40 s. At the voltage higher than 2.1 V, the nebulization of the solution was too intensive. At the voltage lower than 1.8 V, the time necessary for the nebulization substantially increased. To stabilize ICP after the arrival of the solvent between the steps of sample drying and analyte nebulization, no voltage was applied to the cell for 10 s. As we worked with solutions of inorganic substances, the pyrolysis step was omitted. At the nebulization step, all elements to be determined must simultaneously arrive at the ICP. To attain this, within the time range from 55 to 65 s of the temperature program, a voltage of 16 V close to the maximum possible one was applied to the cell. At the purification step even at the greatest possible voltage applied to the cell (17 V), no ASs from the analytes were observed. The parameters of the temperature program chosen for the work are listed in Table 2.

To check the completeness and synchrony of the arrival of analytes with different physical and chemical properties at the ICP, we studied the time dependences of the arrival of analytes at the ICP in electrothermal vaporization. In the measurements we used multielement solutions prepared on the basis of MES solutions with concentrations of the majority of analytes about

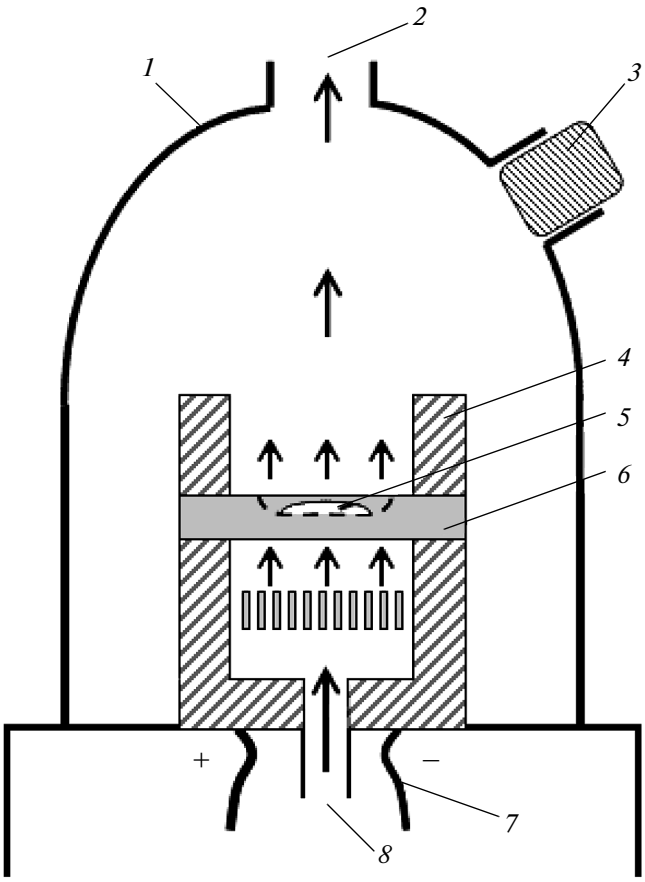

Fig. 1. Block diagram of device for the electrothermal vaporization of samples: *1*, glass cover; *2*, pipe for sample transport to ICP; *3*, hole for sample introduction; *4*, holders; *5*, sample; *6*, graphite cell; *7*, power supply unit; *8*, transport argon flow.

1 μg/mL. It was found that, at the chosen temperature program, Ag, Al, Ba, Be, Bi, Cd, Co, Cr, Cu, Fe, Ga, In, Mg, Mn, Ni, P, Pb, Re, Sb, Se, Sn, Ti, V, and Zn quantitatively arrived at the ICP. As an example Fig. 2 presents the time dependences of analytical signals from Cd, Ga, and Re. It can be seen that, even for elements with considerably differing melting (29.7°C for Ga, 3180°C for Re) and boiling (776°C for Cd, 5600°C for Re) points and, correspondingly, saturated vapor pressures, the times of arrival at the ICP under the chosen ETA conditions were almost equal.

Table 2. Temperature program of electrothermal vaporization

Heating step	Duration, s	Voltage, V
Sample drying	45	1.8
Pause	10	0
Analyte vaporization	10	16

Optimization of the transporting gas flow and the power of the ICP. It is known that the flow of the transporting gas affects both the analytical and the background signal [10,11]. The flow rate of argon was varied in the range 0.1–2.0 L/min. It can be seen in Fig. 3 that, for different elements, the maximum AS-to-background ratio was obtained at different flow rates of the transporting gas.

Table 3 summarizes data on elements, spectral lines, and corresponding ranges of flow rates of the transporting gas at which the maximum AS-to-background ratios were attained. Transporting gas flow rate of 0.6 L/min, at which the AS-to-background ratio for the majority of the used spectral lines of analytes was the maximum, was found to be optimum.

Table 4 illustrates the influence of the ICP power in a range from 750 to 1350 W on the AS-to-background ratio for a number of spectral lines. It follows from Table 4 that this ratio for different lines obtained a maximum at different values of ICP power and that the highest power not always ensures a maximum in the AS-to-background ratio for a number of spectral lines, because with increasing power, the growth of the background signal exceeds that of AS. For the majority of analytical lines, the AS-to-background ratio obtained a maximum at the power in a range from 1150 to 1350 W; therefore, the further measurements were performed at the power 1250 W.

Comparison of electrothermal vaporization and pneumatic nebulization of sample solutions into ICP. It was of interest to study the effect of the method of sample introduction to the ICP on the value of the analytical signal for the elements to be determined, the background signal, and the AS-to-background ratio. The measurements were performed using multielement solutions with analyte concentrations of about 0.1 μg/mL. The parameters of pneumatic nebulization are listed in Table 1. The results of measurements are presented in Table 5.

From the data presented in Table 5 we can draw the following conclusions:

(1) Under the chosen conditions of ETV-ICP-AES analysis, the value of the AS for the majority of elements is ~70% of its value at the pneumatic nebulization;

(2) For three elements Al, Cu, and Ti, a higher analytical signal is observed at electrothermal vaporization;

(3) The level of the background signal in electrothermal vaporization is, on an average, 10 times lower, which is, probably, determined by the absence of solvent particles in the ICP during signal registration.

To summarize, we can state that a decrease in the level of background signal at ETV ensures an increase in the AS-to-background ratio in comparison to the pneumatic nebulization of solutions, on an average, by 6.5 times.

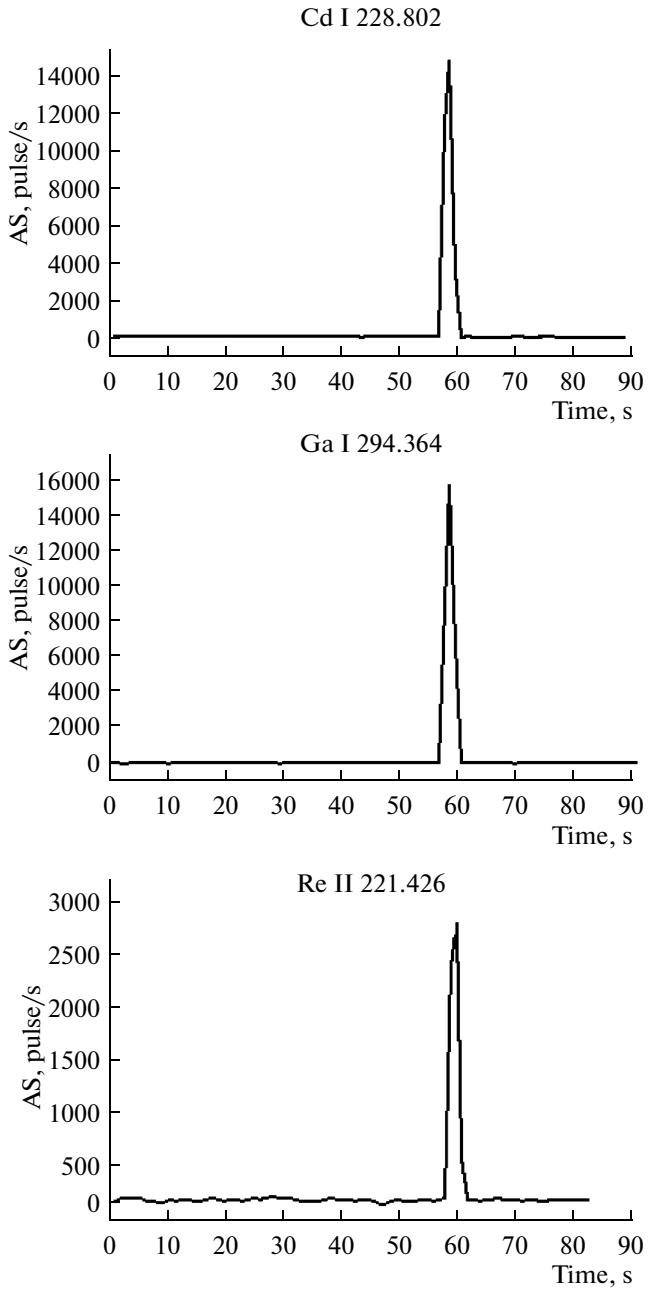

Fig. 2. Delivery of Cd, Ga, and Re into ICP as a function of time in electrothermal vaporization (I are atomic lines, II are ionic lines).

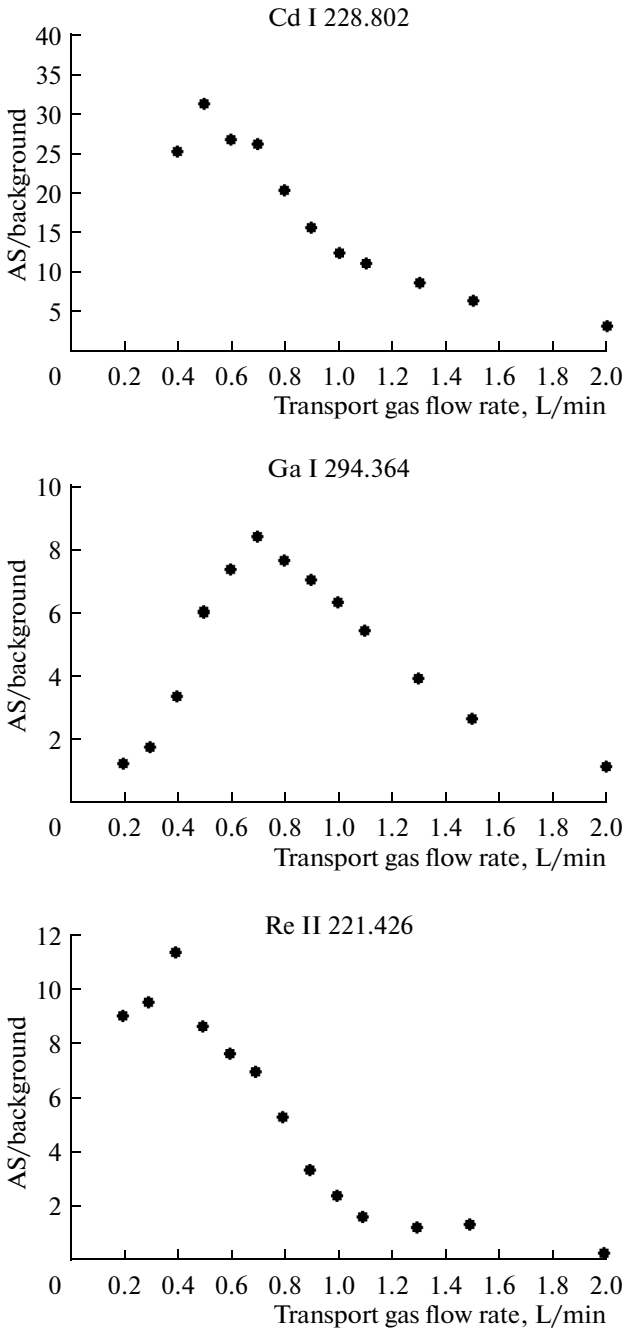

Fig. 3. Effect of the flow rate of transport gas on the ratio of the analytical signal to the background signal for spectral lines Cd I 228.802, Ga I 294.364, and Re II 221.426.

Comparison of the analytical characteristics of AES procedures using direct-current arc (DCA AES), ICP-AES, and ETV-ICP-AES of the analysis of nitric acid solutions with impurity preconcentration by evaporation. In ICP-AES analysis solid samples are most often for transferred into solution using nitric acid. This is, first, due to the solubility of the majority of analytes in HNO_3 and, second, due to the possibility of preparing high-purity nitric acid. The limits of detection were estimated by the $3s$ +BE-test, where s is the standard deviation of the signal of the blank experiment and BE is the signal of the blank experiment ($n = 10$). The calibration dependences were built using multielement solutions prepared from standard MES solutions. The preconcentration of impurities in 6 M HNO_3 twice-purified by distillation under the boiling point was performed by the evaporation of

Table 3. Groups of elements with the maximum AS-to-background ratio at the specified flow rates of transport gas

Analyte and line type, λ, nm	Transport gas flow rate, L/min
Al II, 281.619; Re II, 221.426	0.1–0.4
Ag I, 328.068; Bi I, 223.061; Cd I, 228.802; Co II, 228.616; Cr II, 283.563; Fe II,259.940; Ga I, 294.364; In II, 230.606; Ni I, 300.249; Sb I, 206.833; Sn I, 242.949; Ti II, 334.941; V II, 309.311; Zn I, 213.856	0.5–0.7
Be II, 313.042; Cu I, 324.754; Mn II, 257.610; P I, 213.618	0.8–1.0

Table 4. AS-to-background ratio for spectral lines as a function of ICP power

Line type, λ, nm	ICP power, W						
	750	850	950	1050	1150	1250	1350
Ag I, 328.068	4.6	6.1	7.6	8.3	7.8	7.4	6.8
Al II, 281.619	0.0	0.0	0.2	0.3	0.3	0.7	2.6
Bi I, 223.061	5.0	5.9	7.4	8.9	8.3	9.0	11
Cd I, 228.802	12	18	25	27	32	34	35
Co II, 228.616	10	20	24	31	32	34	35
Fe II, 259.940	19	29	39	43	48	46	41
Ga I, 294.364	5.3	7.0	7.4	6.7	6.0	5.1	4.6
In II, 230.606	2.6	3.3	3.4	3.2	2.8	2.4	2.1
Ni I, 231.398	4.5	7.1	8.3	10	11	11	11
Ni I, 300.249	4.3	4.4	3.7	3.7	3.1	2.7	2.4
P I, 213.618	3.2	3.2	4.2	3.7	3.7	3.2	2.8
Pb II, 220.353	1.5	3.2	4.2	4.4	4.7	4.9	4.6
Re II, 221.426	3.2	4.4	7.3	7.7	8.3	7.0	7.5
Sb I, 206.833	1.3	1.7	2.3	2.8	2.5	2.7	2.5
Sn I, 242.949	2.6	3.3	3.5	3.5	2.8	2.6	2.3
Sn I, 283.999	2.6	3.5	3.4	3.6	3.5	3.2	3.1
Ti II, 334.941	9.0	9.7	9.3	9.4	7.8	7.1	7.1
V II, 309.311	2.5	2.8	3.8	4.6	4.4	4.1	4.6
Zn I, 213.856	12	23	27	40	45	51	51

a 2-mL aliquot portion of the acid under an IR lamp in a forced-draft chamber.

In DCA AES analysis, an impurity concentrate was evaporated on a substrate made from 50 mg of spectral graphite powder (high-purity brand 8-4, GOST 23463-79) with an intensifying additive of NaCl high-purity brand 6-4, TU 6-05-3658-74, 4%). DCA spectra at a current of 13.5 A were recorded on a PGS-2 diffraction grating spectrometer (600 lines/mm) [2]. The calibration graphs were built using the Atom 2.10 software (MAES) and reference materials on the basis of graphite powder containing 4% NaCl prepared from SGP 27 pr. GSO 2820-83 (OSO 48-4-39-94) by successive dilutions.

At ICP-AES analysis, a 2-mL sample was evaporated in a fluoroplastic cup under an IR lamp in a forced-draft chamber to a volume of ~25 μL and then diluted to 2 mL with deionized water. Calibration dependences were built using solutions prepared from MES solutions. The internal standard was Sc. The spectra were recorded on an iCAP 6500 ICP-AES a

Table 5. Comparison of the analytical signal, background signal, and their ratio in the electrothermal vaporization of samples into ICP and in the pneumatic nebulization of solutions

Line type, λ, nm	$AS_{ETV}/AS_{pneumatic\ neb.}$	$Background_{ETV}/Background_{pneumatic\ neb.}$	$AS/Background_{ETV}/AS/Background_{pneumatic\ neb.}$
Ag I, 328.068	1.0	0.10	10
Al I, 396.152	1.6	0.10	16
Be I, 234.861	0.48	0.09	5.3
Be II, 313.042	0.34	0.11	3.1
Be II, 313.107	0.36	0.11	3.3
Cd I, 228.802	0.32	0.09	3.6
Co II, 228.616	0.26	0.09	2.9
Cr II, 283.563	0.39	0.10	4.0
Cu II, 219.226	0.31	0.09	3.4
Cu I, 324.754	1.8	0.10	18
Fe II, 259.940	0.51	0.10	5.1
Ga I, 294.364	1.0	0.10	10
In I, 325.609	0.91	0.10	9.1
Mn II, 257.610	0.43	0.09	4.8
Ni II, 231.604	0.30	0.09	3.3
Ni I, 300.249	0.89	0.10	8.9
Pb II, 220.353	0.19	0.10	1.9
Re II, 221.426	0.21	0.10	2.1
Sn I, 283.998	0.42	0.10	4.2
Ti II, 334.941	2.1	0.14	15
V II, 309.311	0.72	0.11	6.6
Zn I, 213.856	0.31	0.09	3.4
Average value	0.67	0.10	6.5

spectrometer at a plasma power of 1150 W and the rate of solution delivery 1.5 mL/min.

In ETV-ICP-AES analysis, a 2-mL sample was evaporated similarly to a volume of 20–30 μL followed by the analysis of the concentrate obtained.

Table 6 presents the limits of detection in the analysis of nitric acid twice-cleared by distillation under the boiling point by DCA AES, ICP-AES, and ETV-ICP-AES with the preconcentration of impurities. Note that, for different methods, the positions of the analytical lines are different, which is due to difference in the spectral ranges of the instruments used (DCA and ICP-AES) and in the conditions of sample introduction to the plasma (pneumatic nebulization or electrothermal vaporization). DCA AES and ICP-AES methods with pneumatic nebulization of solutions can determine more elements compared to ETV-ICP-AES. This is explained by the restriction of the highest possible temperature of heating graphite cells in the P.S. Analytical 60.800 instrument, preventing the determination of elements such as W and Zr. In ICP-AES analysis, the range of determinable elements also covers K, Li, Na, Sr, and Te (LODs are at a level of $n \times 10^{-9}$–$n \times 10^{-6}$). The lowest LODs are attained in ETV-ICP-AES, which is due to the high value of the preconcentration factor (80) and a more efficient source of spectrum excitation compared to DCA (for DCA AES $K_{conc} = 40$ and for ICP-AES $K_{conc} = 1$).

Table 7 presents the results of ETV-ICP-AES analysis of high-purity HNO_3 brand 27-5 (NAK Nitrogen Open Society, Novomoskovsk, batch 17 from September, 2012). The procedure of sample preparation and the conditions of analysis corresponded to those used in the analysis of HNO_3 purified by distillation under the boiling point, except for the initial sample volume being 1 mL. As can be seen in Table 7, the concentration of Cu exceeds the requirements of GOST (State Standard) 11125-84, which can be due to uncontrolled pollution in performing the analysis and the concentrations of Al, Fe, and Mg are at a level of GOST requirements. Thus, the study performed has shown that ETV-ICP-AES ensures considerably lower

Table 6. Limits of detection (wt %) for impurity elements in nitric acid twice-purified by distillation under the boiling point using DCA AES, ICP-AES, and ETV-ICP-AES methods with preconcentration (estimated by the $3s$ + BE test, $n = 10$)

Element	DCA AES		ICP-AES		ETV-ICP-AES	
	λ, nm	LOD	λ, nm	LOD	λ, nm	LOD
Ag	328.068	3×10^{-8}	328.068	2×10^{-7}	328.068	8×10^{-10}
Al	308.215	3×10^{-7}	396.152	2×10^{-7}	396.152	3×10^{-9}
Ba	233.527	3×10^{-6}	455.403	1×10^{-8}	233.527	5×10^{-9}
Be	234.861	3×10^{-8}	313.107	2×10^{-8}	234.861	8×10^{-10}
Ca*	317.933	3×10^{-6}	393.366	1×10^{-6}	–	–
Cd	228.802	1×10^{-7}	226.502	3×10^{-8}	228.802	3×10^{-9}
Co	242.493	5×10^{-7}	228.616	1×10^{-7}	228.616	5×10^{-8}
Cr	284.324	5×10^{-7}	267.716	1×10^{-7}	283.563	3×10^{-9}
Cu	324.754	5×10^{-8}	324.754	2×10^{-7}	219.226	2×10^{-8}
Fe	302.064	7×10^{-7}	238.204	2×10^{-7}	259.940	8×10^{-9}
Ga	265.117	8×10^{-8}	287.424	1×10^{-6}	294.364	5×10^{-9}
In	325.609	1×10^{-7}	–	–	325.609	1×10^{-8}
Mg*	280.270	3×10^{-7}	280.270	2×10^{-9}	279.553	1×10^{-7}
Mn	280.108	3×10^{-8}	257.610	1×10^{-8}	257.610	1×10^{-9}
Mo	317.035	3×10^{-7}	202.030	1×10^{-7}	–	–
Ni	305.081	7×10^{-6}	231.604	1×10^{-7}	231.398	5×10^{-8}
P	214.914	3×10^{-5}	213.618	5×10^{-6}	214.914	1×10^{-7}
Pb	283.305	3×10^{-7}	216.999	3×10^{-6}	220.353	1×10^{-8}
Re	–	–	–	–	221.426	8×10^{-9}
Sb	259.807	2×10^{-6}	–	–	206.833	6×10^{-8}
Se	–	–	196.090	3×10^{-6}	241.350	3×10^{-7}
Si*	288.157	8×10^{-6}	251.611	1×10^{-6}	–	–
Sn	283.999	3×10^{-7}	242.949	2×10^{-6}	283.999	2×10^{-8}
Ti	308.803	3×10^{-7}	334.941	2×10^{-8}	334.941	5×10^{-9}
V	318.399	3×10^{-7}	292.402	1×10^{-7}	309.311	4×10^{-10}
W	294.699	1×10^{-5}	239.709	2×10^{-6}	–	–
Zn	213.856	3×10^{-7}	202.548	2×10^{-7}	213.856	3×10^{-8}
Zr	327.927	3×10^{-7}	343.823	1×10^{-7}	–	–

* LOD is limited by the value of the blank experiment.

Table 7. Results of analysis of high-purity nitric acid brand 27-5 by ICP-AES and ETV-ICP-AES with impurity preconcentration ($n = 4$, $P = 0.95$)

Element	ETV-ICP-AES		GOST 11125-84 (no more than, wt %)
	λ, nm	found, wt %	
Ag	328.068	Not found	2×10^{-7}
Al	396.152	$(0.9 \pm 0.2) \times 10^{-6}$	1×10^{-6}
Cd	228.802	Not found	5×10^{-7}
Co	228.616	Not found	5×10^{-7}
Cr	283.563	$(0.9 \pm 0.2) \times 10^{-7}$	8×10^{-7}
Cu	324.754	$(2.8 \pm 0.5) \times 10^{-7}$	2×10^{-7}
Fe	259.940	$(8 \pm 2) \times 10^{-7}$	1×10^{-6}
Mg	382.935	$(1.2 \pm 0.3) \times 10^{-6}$	1×10^{-6}
Mn	257.610	$(6 \pm 1) \times 10^{-8}$	2×10^{-7}
Ni	231.398	Not found	5×10^{-7}
P	214.914	Not found	1×10^{-6}
Pb	220.353	Not found	5×10^{-7}
Sb	206.833	Not found	1×10^{-6}
Sn	283.999	Not found	2×10^{-7}
Ti	334.941	Not found	5×10^{-7}
Zn	213.856	$(1.3 \pm 0.3) \times 10^{-7}$	5×10^{-7}

LODs for impurity elements in HNO_3 (by two orders of magnitude) in comparison to GOST requirements.

ACKNOWLEDGMENTS

We are grateful to V.G. Pimenov (Institute of Chemistry of High-Purity Substances, Russian Academy of Sciences) for technical and methodological assistance. This work was supported by the Presidium of the Russian Academy of Sciences, Program 9, project 2 "Elaboration and Improvement of Informative Procedures of Chemical Analysis for Pure Substances and Functional Materials."

REFERENCES

1. Shelpakova, I.R. and Saprykin, A.I., *Usp. Khim.*, 2005, vol. 74, no. 11, p. 1106.
2. Shelpakova, I.R., Chanysheva, T.A., Tsygankova, A.R., Rodionov, S.G., Troitskii, D.Yu., Petrova, N.I., and Saprykin, A.I., *Zavod. Lab. Diagn. Mater.*, 2007, vol. 73.
3. Lipatova, M.M. and Pimenov, V.G., *Abstracts of Papers*, *ICAS-2006 Int. Congress of Analytical Sciences*, Moscow, 2006, vol. 1, p. 35.
4. Tsygankova, A.R., Shelpakova, I.R., Shestakov, V.A., and Saprykin, A.I., *Zavod. Lab. Diagn. Mater.*, 2010, vol. 76, no. 9, p. 3.
5. Shelpakova, I.R., Saprykin, A.I., Chanysheva, T.A., and Yudelevich, I.G., *Zh. Analyt. Khim.,* 1983, vol. 38, no. 4, p. 581.
6. Chanysheva, T.A., Shelpakova, I.R., Saprykin, A.I., Yankovskaya, L.M., and Yudelevich, I.G., *Zh. Analyt. Khim.*, 1983, vol. 38, no. 6, p. 979.
7. Moens, L., Veppert, T., Boonen, S., Vanhaeske, F., and Dams, R., *Spectrochim. Acta B*, 1995, vol. 50, nos. 4–7, p. 463.
8. Man'shina, I.V., Molodyk, A.D., and Potepalov, V.P., *Vysokochist. Veshchestva*, 1990, no. 1, p. 154.
9. Matusiewicz, H. and Fricke, F.L., *J. Anal. Atom. Spectrom.*, 1986, vol. 1, p. 203.
10. Zilbershtein, Kh.I., *Spektral'nyi analiz chistykh veshchestv* (Spectral Analysis of High Pure Substances), Sankt Petersburg: Khimiya, 1994.
11. Aeschliman, D.B., Bajic, S.J., Baldwin, D.P., and Houk, R.S., *J. Anal. Atom. Spectrom.*, 2003, vol. 18, p. 1008.

Translated by E. Rykova